Reprint of contributed paper to the 3rd Symposium on Linear Drives for Industrial Applications
LDIA 2001, Nagano Japan, pp. 332-336.

Control of a Linear Drive Test Stand for the NBP Railway Carriage

Markus Henke, Horst Grotstollen

Department of Electrical Engineering and Information Technology

FB14/250, University of Paderborn

Warburger Str. 100, 33098 Paderborn, GERMANY

Phone: +49-5251-603653, Fax: +49-5251-603443

E-Mail : henke, grotstollen@lea.upb.de

Abstract

In this paper the control of a test stand for the linear drive of a railway car is described. The modelling of the drive is followed by an analysis of the emerged equations. A control concept has been developed which is oriented at the stator current vector. Therefore precise force control and comfortable longitudinal vehicle dynamics can be assured. A major problem in control of linear motors is the extraction of the vehicle position. A technique to calculate this position by using test signals is presented. There the special features of the doubly fed linear motor are made use of.

Key words: Linear Drives, Modelling, Control, NBP

1 Introduction

At the University of Paderborn a mechatronic railway vehicle, driven by a longstator linear motor is designed. The basic concept of the NBP project (Neue Bahntechnik Paderborn)[1] is to realize the drive function by way of a linear drive integrated into the existing rail system. By using active suspension/tilt technology the ride comfort will be improved and in combination with an active steering device, the wear of wheels and rails will be minimized. The technology is embedded into an overall logistical structure and a fully automated shuttle is built up useable for the transport both of passengers and goods. The vehicles operate without magnetic levitation in order to use the simple structure of the existing railway lines [1].

2 Propulsion module

To operate shuttles in convois of different size, it is necessary to control several vehicles on the same stator segment. The control of the longitudinal motion in general can only be done by the primary (conventional linear longstator motor).

Another main objective of the NBP shuttle is to operate without power transmission lines and without current collectors. Furthermore the shuttles should be able to accelerate and decellerate at any position, they especially should be able to build convois. This can be realized via rendezvous maneuvers between several seperated shuttles.

For this reasons, three-phase windings are implemented in the secondary. With this doubly fed linear motor design, it is possible to align the excitation field in the secondary at will, so that the force generation is optimized and several shuttles can perform different thrust forces on the same stator segment [2].

3 Test stand

The testing of the drive module is done on a test stand of 8 m in lenght and a vehicle of 187 kg weight. The maximum thrust force is about 500 N with an air gap of 9 mm.

The longstator is devided into two seperately supplied parts. Therefore the switching between stator segments and the entering of the secondaries can be studied. The three-phase windings of the secondaries are also devided into two parts because of an additional pitch control [3]. All servo controllers communicate with the host PC via a DSP board.

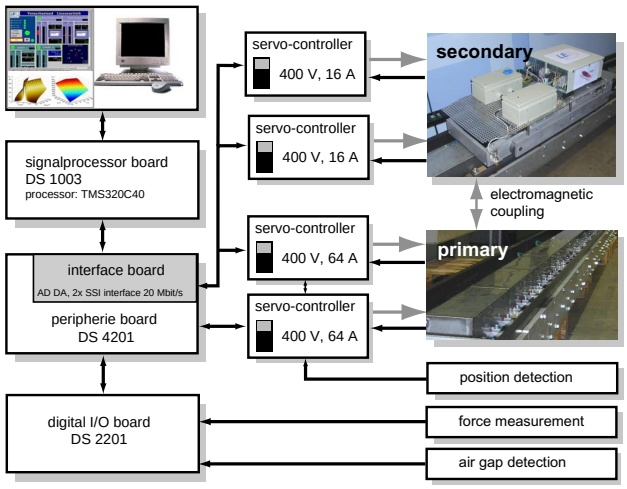

Figure 1. Test stand for the doubly fed linear drive

On the test stand the vehicle position can be detected with an incremental encoder on a steel coil up to 0.05 mm. The velocity is gained via differentiation of the position signal. The air gap is measured by two separate sensor systems, a laser system and an eddy current system. The test

1.The project NBP (Neue Bahntechnik Paderborn) is sponsored by the federal state of North Rhine Westphalia and by the University of Paderborn

stand is also fitted with force sensors to measure thrust forces.

3.1 Modelling of the test stand

To analyse the dynamical behaviour of the linear drive the mathematical equations of the whole system have to be set up, comprising voltage and force equations. All parts of the system should be calculated in a common coordinate system. The orientation on the stator flux linkage depends on the excitation of each secondary, so that a lot of communication between the shuttles would be necessary. Here the orientation on the stator *current* vector is used, so that the coordinate system moves along with the position of the stator field [2]. Fig. 2 shows the vectors of a system with two secondaries. Secondary 1 moves along with the velocity v_{m1} and the stator field velocity is v_{KS}, representing the relative movement between the coordinate system K and the stator. So the frequency of the secondary currents in secondary 1 is ω_{KL1} . The slip is calculated by

$$s_1 = \frac{\omega_{L1}}{\omega_S} = \frac{\omega_S - \omega_{LS1}}{\omega_S} = \frac{v_S - v_{LS1}}{v_S} \qquad (1)$$

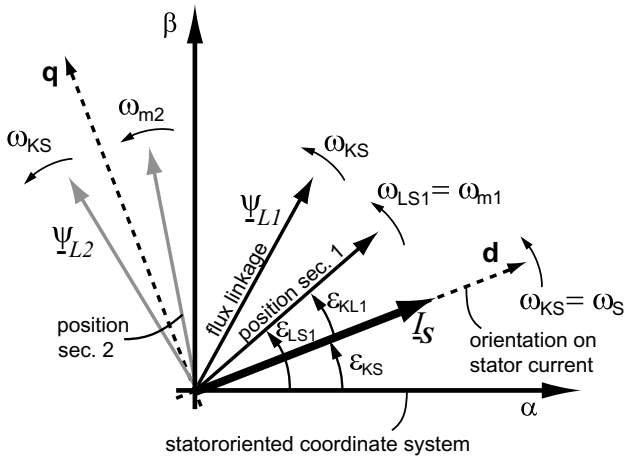

Figure 2. Coordinate System

Because there are two primaries and two secondaries in the test stand, four coupling inductivities have to be considered (Fig. 3).

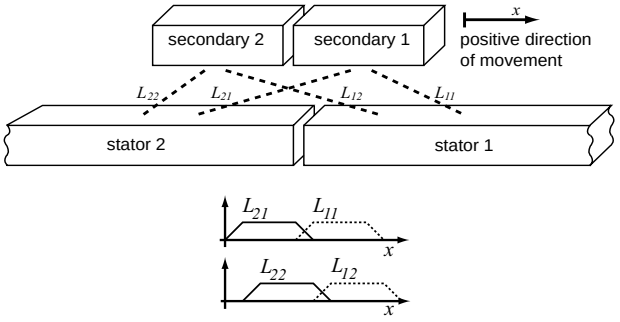

Figure 3. Coupling inductivities on the test stand

Their values depend on the vehicles position. The coupling inductivities $L_{ij}(x)$ increase linearly when the secondary enters or leaves the active primary section. This effect has to be taken into account by controlling the motor because it directly effects the force buildup.

There are also Nonlinearities emerging from the stator design which have to be taken into account as well. The endpoles of the motorelements are fitted with less windings, sothat the coupling inductivity decreases, also depending on the vehicle position.

To set up the system equations it is useful to regard the equivalent cirquit of the linear motor (fig. 4). The inductivities and resistances are shown clearly and the nonlinear behaviour can be integrated easily by variing parameters for the coupling inductivities. The dashed values are related to the primary side of the motor.

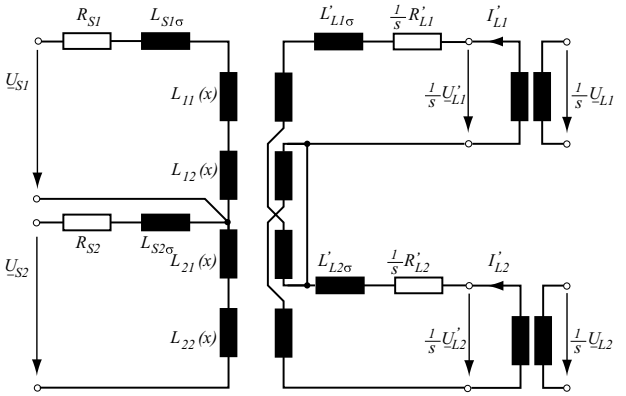

Figure 4. Equivalent cirquit of the test stand

The inductivities are calculated as

$$\begin{aligned} L_{S1} &= L_{S\sigma 1} + L_{11} + L_{12} \\ L_{S2} &= L_{S\sigma 2} + L_{21} + L_{22} \end{aligned} \qquad (2)$$

The flux linkages of the primaries can be calculated with the use of primary and secondary currents as

$$\begin{aligned} \underline{\Psi}_{S1} &= L_{S1} \cdot \underline{i}_{S1} + L_{11} \cdot \underline{i}'_{L1} + L_{12} \cdot \underline{i}'_{L2} \\ \underline{\Psi}_{S2} &= L_{S2} \cdot \underline{i}_{S2} + L_{21} \cdot \underline{i}'_{L1} + L_{22} \cdot \underline{i}'_{L2} \end{aligned} \qquad (3)$$

The equation shows the influence of the secondaries to the flux linkages. The coupling is represented by the coupling inductivities L_{11} and L_{12} and by the secondary currents $\underline{i}_{L1}$ and $\underline{i}_{L2}$.

The flux linkage of the secondaries can be calculated as follows

$$\begin{aligned} \underline{\Psi}_{L1} &= L_{L1} \cdot \underline{i}'_{L1} + L_{11} \cdot \underline{i}_{S1} + L_{21} \cdot \underline{i}_{S2} \\ \underline{\Psi}_{L2} &= L_{L2} \cdot \underline{i}'_{L2} + L_{12} \cdot \underline{i}_{S1} + L_{22} \cdot \underline{i}_{S2} \end{aligned} \qquad (4)$$

To determine the voltage equations the time derivative of (3) and (4) has to be set up.

It is assumed, that the stator current ampliutude remains nearly constant while operation, whereas the forcecontrol is realized via the secondary currents. So the time derivative of the stator current vector equals zero, due to the orienta-

tion of the coordinate system on i_{Sd}.

The statorcurrent equation results in

$$\frac{d\underline{i}_{S1}}{dt} = \frac{\underline{u}_{S1}}{L_{S1}} - \frac{R_{S1}}{L_{S1}}\underline{i}_{S1}$$
$$- \frac{L_{11}}{L_{L1}L_{S1}}(\underline{u}'_{L1} - R'_{L1}\underline{i}'_{L1} - j\omega_{KL}(L_{L1}\underline{i}'_{L1} + L_{11}\underline{i}_{S1} + L_{21}\underline{i}_{S2}))$$
$$- \frac{L_{12}}{L_{L2}L_{S1}}(\underline{u}'_{L2} - R'_{L2}\underline{i}'_{L2} - j\omega_{KL}(L_{L2}\underline{i}'_{L2} + L_{12}\underline{i}_{S1} + L_{22}\underline{i}_{S2}))$$
$$- j\omega_{KS}\frac{1}{L_{S1}}(L_{S1}\underline{i}_{S1} + L_{11}\underline{i}'_{L1} + L_{12}\underline{i}'_{L2}) \quad (5)$$

The complex currents of the secondaries are calculated as

$$\frac{d\underline{i}'_{L1}}{dt} = \frac{1}{L_{L1}}(\underline{u}'_{L1} - R'_{L1}\underline{i}'_{L1} - j\omega_{KL}(L_{L1}\underline{i}'_{L1} + L_{11}\underline{i}_{S1} + L_{21}\underline{i}_{S2}))$$
$$\frac{d\underline{i}'_{L2}}{dt} = \frac{1}{L_{L2}}(\underline{u}'_{L2} - R'_{L2}\underline{i}'_{L2} - j\omega_{KL}(L_{L2}\underline{i}'_{L2} + L_{12}\underline{i}_{S1} + L_{22}\underline{i}_{S2})) \quad (6)$$

These equations now can be easily transformed into statorcurrent orientated coordinates d,q by using the transformation angle ε_{KS} .

The force-buildup depends on the coupling inductivitites and the currents in primary and secondary. Here the force equation is proportional to the orthogonal components of the primary and secondary current in d- and q- axis.

$$F_m = -\frac{3\pi}{2\tau_p}(L_{11}i_{L1q}i_{S1d} + L_{12}i_{L2q}i_{S1d} + L_{21}i_{L1q}i_{S2d} + L_{22}i_{L2q}i_{S2d}), \quad i_{L1,2d} = 0 \quad (7)$$

Because of the mechanical structure of the linear motor and the resulting non-sinusodal distribution of ampere-turns per cm the force is effected by harmonics. These harmonics have been identified by measuring coupling inductivities and are implemented in the motormodel as a position variant fourier series. Fig. 5 shows the verification of that approach. The experimental and the simulated results differ only about 2 %.

4 Control scheme

The control of the linear motor can be structured in current control for primary and secondary, velocity control and position control.

4.1 Stator current control

Contrary to conventional linear drive systems, the stator represents a unit whose current has to be controlled as to constant frequency and amplitude during operation. The frequency depends on the vehicle velocities and effects the energy flow between stator and secondary which can be controlled seperately in upper cascaded control loops [4]. The energy flow between stator and secondary can be analysed via currents and voltages in primary and secondary.

Several vehicles on the same stator segment are magnetically coupled via the stator. Disturbances in stator current control are the voltages induced by several shuttles operating on the same segment and error voltages resulting from the feeding converter.

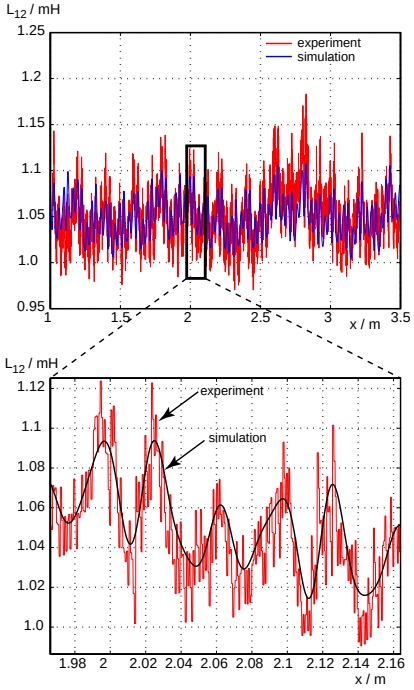

Figure 5. Simulation of nonlinear coupling inductivities

4.2 Motion control

The longitudinal dynamics of each coach are controlled via the electrical position of the secondary current . All shuttles use the common stator flux. The switching between different statorsegments is taken into account and the segments the shuttle is running into have to build up the current just before the secondary enters the segment.

As the stator current component $i_{S1,2d}$ is fixed at a constant value, the only remaining actuating variable for thrust control is the q-component of the secondary current $i_{L1,2q}$ (7).

The actual values of the current components are directly determined by transforming the measured primary and secondary currents.

For the control of the carriage (fig. 6), there are thus three remaining variables to be controlled: the components of the secondary current and, superordinated, the velocity of each carriage. All these control loops are realized with PI-controllers. The decoupling structure is used to decouple the d- and q-loops of the secondary currents. Feedforward control of velocity and secondary current yields a reduction of the position error.

A simulation model has been realized for the control shown above. It includes the cascaded vehicle control and the power management of two shuttles, operating on the same stator segment.

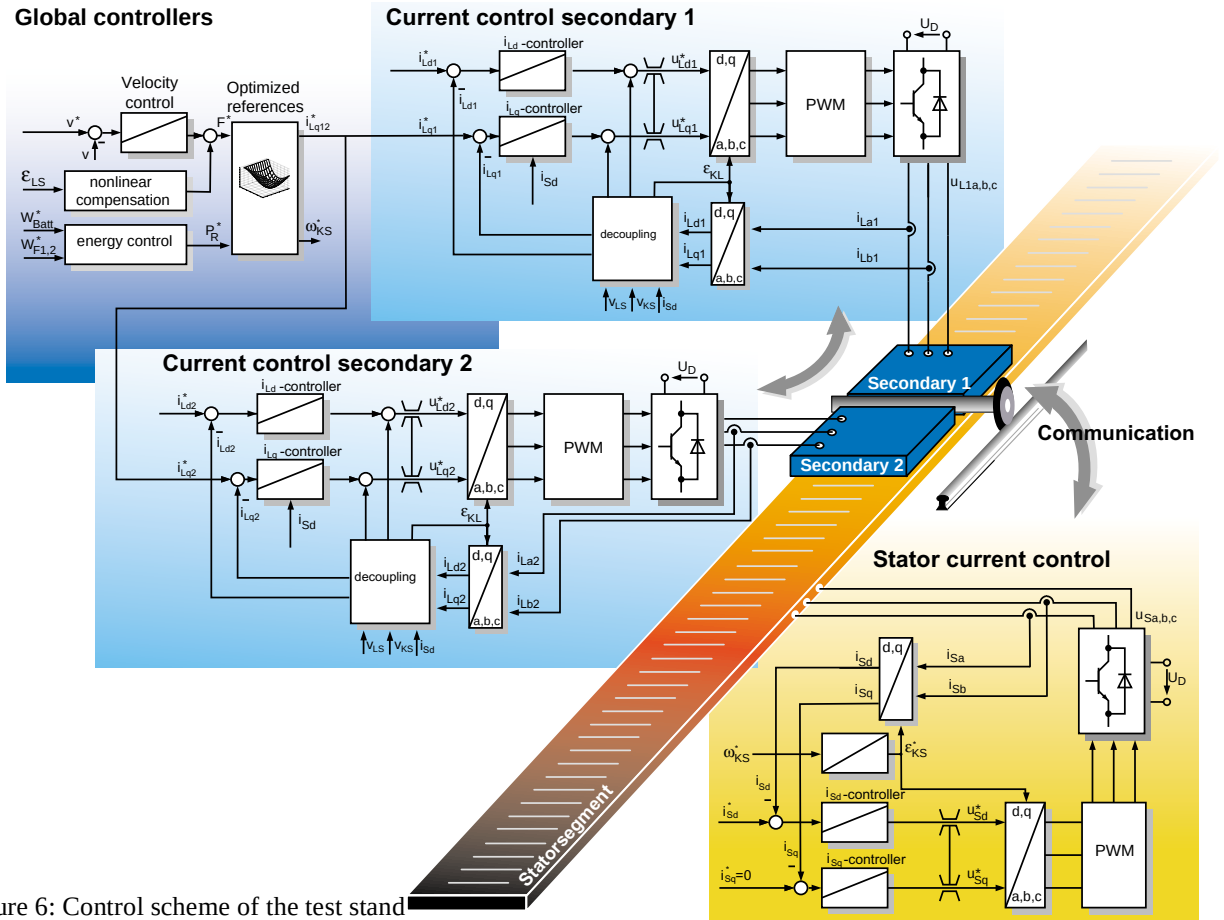

Figure 6: Control scheme of the test stand

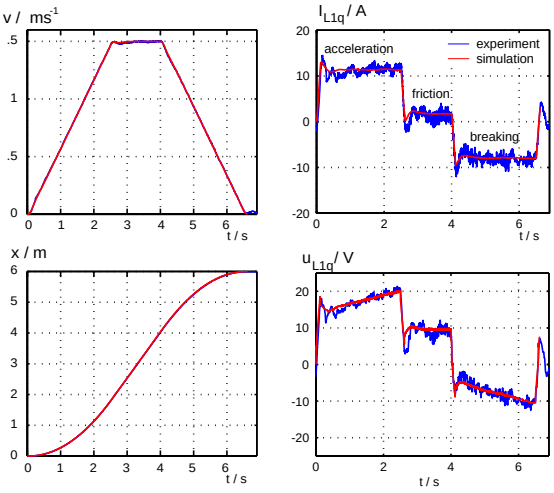

Figure 7: Experimental Results of position control

In fig. 7. the reference profile for position and velocity is shown and the resulting secondary currents. The motor accelerates up to 1.5 m/s and decellerates with a maximum position error of about 5 mm.

5 Sensorless position control

The NBP railway vehicle needs a position detection device on board to determine the relative position x_{KL} of the vehicle respective to the stator field. Another possibility is to calculate the position with the help of a sinusoidal testsignal. One main advantage is that the parameters of the drive like the inductivities, the airgap and resistances do not effect the calculation. Here a test signal of high frequency is added to the stator current, the vehicle position can be calculated from the voltage induced in the windings of secondary 1. The signal has to be oriented on the known stator current vector and is here added to the q-component of the stator current, so that there is no effect on the thrust force because of the control law $i_{L1,\,2d} = 0$. The effect can be calculated by

$$\underline{i}_{S1} = \underline{i}_{S10} + \underline{\tilde{i}}_{S1} = i_{S10} \cdot e^{j\omega_{KL}t} + \tilde{i}_{S1}\cos(\omega_{test}t) \cdot e^{j\pi/2} \quad (8)$$

To avoid extensive voltage measuring, the voltage reference values $u^*_{L\alpha,\,\beta}$ are used for position detection. A high-pass filter and a following atan-algorithm determine the position in the interval $\pm\pi/2$, so that a counter is implemented to add the actual number of angle cycles.

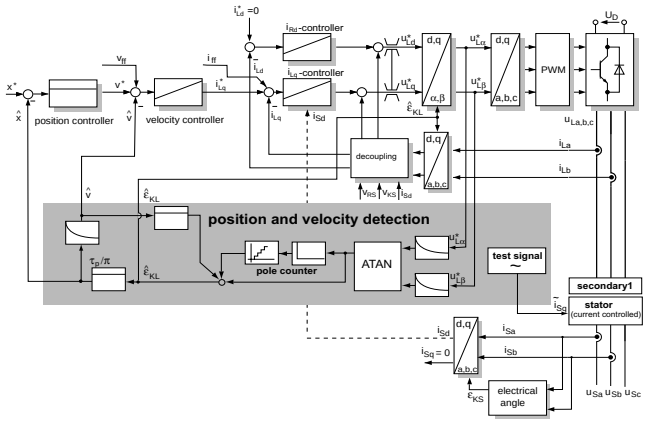

Figure 8: Structure of the sensorless control scheme

5.1 Experimental results

Fig. 9 shows the results of sensorless closed loop position control. At *t=5* s a load step affects the system. The position error at that moment is less than 0.01 m at a velocity of 0.8 m/s .

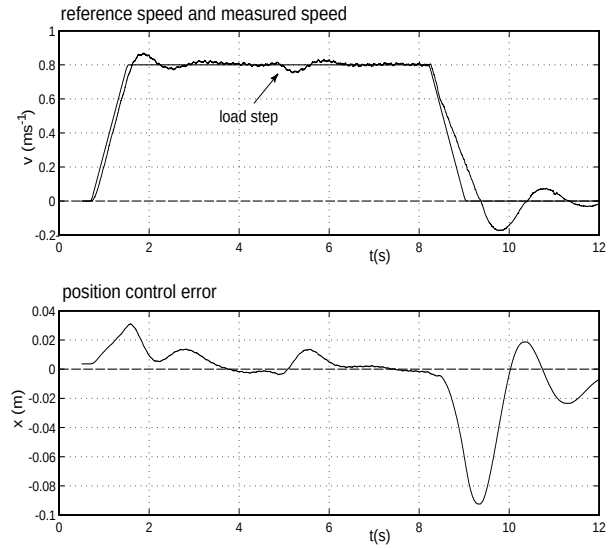

Figure 9: Experimental results of sensorless position control

6 Conclusions

The mathematical model of the presented doubly fed linear drive has been set up and analyzed. Due to the transformation of all state variables into the statorcurrent coordinate system a simple force equation results. The control structure is oriented on these model and the control loops for primary and secondary are presented. The vehicle position, respectively the electrical position of the secondaries can be obtained by the presented sensorless position control scheme. The results suffice the demands on position precision. One main advantage of using a test signal for position estimation is the complete independence from system parameters, which vary during operation.

7 References

[1] J. Lückel; H. Grotstollen; K.-P. Jäker; M. Henke; X. Liu: Mechatronic Design of a Modular Railway Carriage, IEEE/ ASME International Conference on Advanced Intelligent Mechatronics 1999, Atlanta, GA, USA, 1999,pp. 1020-1025.

[2] M. Henke; H. Grotstollen: Modelling and Control of a Longstator-Linearmotor for a Mechatronic Railway Carriage, IFAC Conf. on Mechatronic Systems, MECHATRONICS 2000, Darmstadt, Germany. pp. 353-357

[3] B. Yang, M. Henke, H. Grotstollen: Realization of Pitch Control on the Teststand for NBP Wheel-on-Rail System, LDIA 2001, Nagano, Japan

[4] M. Henke, A. Kathöfer, H. Grotstollen: Simulation von Betriebsverhalten und Energieflüssen des NBP-Linearantriebes, ASIM 2001 Paderborn (german)